J|A|C|S COMMUNICATIONS

Published on Web 12/31/2010

Syntheses and Dynamics of Donor−Acceptor [2]Catenanes in Water

Lei Fang, Subhadeep Basu, Chi-Hau Sue, Albert C. Fahrenbach, and J. Fraser Stoddart*

Department of Chemistry, Northwestern University, 2145 Sheridan Road, Evanston, Illinois 60208-3113, United States

Received September 30, 2010; E-mail: stoddart@northwestern.edu

Abstract: A subset of mechanically interlocked molecules, namely, donor−acceptor [2]catenanes, have been produced in aqueous solutions in good yields from readily available precursors. The catenations are templated by strong hydrophobic and [$\pi\cdots\pi$] stacking interactions, which serve to assemble the corresponding supramolecular precursors, prior to postassembly covalent modification. Dynamic ^{1}H NMR spectroscopic investigations performed on one of these [2]catenanes reveal that the pirouetting motion of the butadiyne-triethylene glycol chain occurs with a dramatically lower activation enthalpy, yet with a much higher negative activation entropy in water, compared to organic solvents. The preparations of mechanically interlocked molecules in water constitute the basis for the future development of complex functional molecular machinery in aqueous environments.

As early as 560 BC, Thales of Miletus had declared[1] that water is the primary essence of nature. Indeed, from a modern scientific perspective, water supports most living organisms on our planet by mediating and regulating complex biological processes. Most biomolecules are controlled with respect to form and function in aqueous solution.[2] Among these biomolecules, almost all the molecular machines—e.g., ATP synthase,[3] kinesin,[4] and myosin[5]—are assembled[6] in aqueous environments and perform work therein. In order to seek a better understanding about the functions of these naturally occurring motor proteins, various model systems, based on artificial molecular machines,[7] have been designed and investigated. Most of these artificial systems are, however, constructed in organic solvents and usually only serve as functional machines in these solvents. Alas, the ubiquitous role of water[2] in biological processes cannot be addressed and appreciated fully by studying only the development of the model systems in nonaqueous solvents. It is therefore important, in this context, to perform both the construction and the investigation of the function of artificial molecular machines in aqueous media. Water, a unique solvent, imposes[8] two formidable challenges. They are (*i*) the solubility characteristics of the organic building blocks in aqueous environments and (*ii*) strong interference[8] by water molecules which tend to disrupt the noncovalent bonding interactions, which are essential to the operation of these artificial molecular machines. In order to address issue (*i*), solubilizing groups are typically attached to the organic building blocks, while electrostatic interactions and hydrophobic surroundings are usually employed to provide efficient noncovalent bonding interactions to address issue (*ii*).

Mechanically interlocked molecules[9] (MIMs) constitute an important family of artificial molecular machines on account of the potential of their components to exercise relative intramolecular motion.[10] The synthesis of MIMs relies for the most part on template-directed protocols,[11] which are typically dominated by noncovalent bonding interactions, e.g., van der Waals forces,[12] [$\pi\cdots\pi$] interactions,[13] hydrogen bonds (H-bonds),[14] and metal coordination.[15] Although water suppresses the H-bonding interactions as a result of its strong H-bond donating and accepting abilities, it facilitates the mutual interactions between nonpolar organic species using the so-called hydrophobic effect. By employing this unique effect, "in-water" syntheses of cyclodextrin-based MIMs have been explored[12,16] widely. Furthermore, donor−acceptor [2]catenanes can also be assembled in aqueous solution using dynamic covalent chemistry—e.g., reversible metal coordination[17] or disulfide bond formation[18]—and a combination of hydrophobic and [$\pi\cdots\pi$] interactions. Herein, we report the kinetically controlled syntheses and characterization of charged donor−acceptor [2]catenanes, followed by the investigation of their dynamic behavior in water.

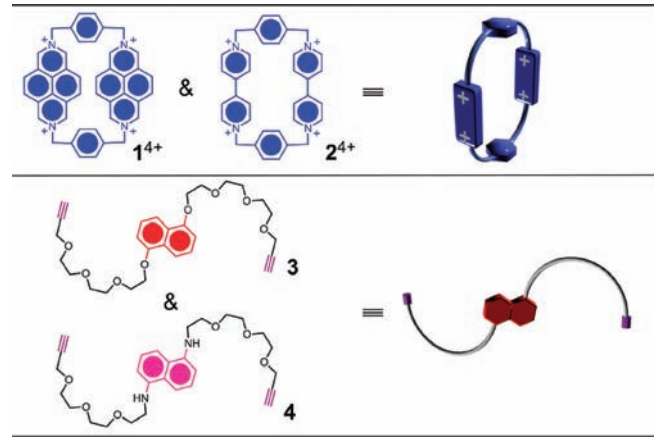

Figure 1. Structural formulas and their graphical representations of the π-electron deficient cyclophanes **1**$^{4+}$ and **2**$^{4+}$, as well as the bispropargyl ethers **3** and **4** of acyclic polyethers incorporating 1,5-dioxy- and 1,5-diaminonaphthalene units, respectively.

The π-electron deficient tetracationic cyclophanes[19] **1**$^{4+}$ and **2**$^{4+}$ are host molecules which can form[20,21] strong donor−acceptor inclusion complexes with π-electron rich guests, e.g., the 1,5-dioxynaphthalene derivative **3**[22] and the 1,5-diaminonaphthalene derivative **4** (Figure 1). Although compounds **1**$^{4+}$ and **2**$^{4+}$ are both rigid rectangular macrocycles, they are composed of different electron-deficient components, namely, diazapyrenium (DAP^{2+}) and bipyridinium (BIPY^{2+}) units, respectively. In this communication, these tetracationic cyclophanes are selected as suitable candidates for assembling MIMs in water using template-directed protocols, primarily because of their water solubility (with $CF_3CO_2^-$ and Cl^- as the counterions, respectively) and unique host−guest properties (*vide infra*).

Inspired by previous reports,[22−24] we have employed (Scheme 1) a threading-followed-by-cyclization approach to generate the corresponding [2]catenanes **5**$^{4+}$−**8**$^{4+}$ in water. This approach relies upon the formation of pseudorotaxanes (e.g., **3**⊂**1**$^{4+}$) prior to the cyclization of the threads, which, in every case, are terminated by bispropargyl functions. The key to being able to carry out the

10.1021/ja1087562

Scheme 1. Syntheses of Donor−Acceptor [2]Catenanes $\mathbf{5}^{4+}$−$\mathbf{8}^{4+}$ in Aqueous Solutions

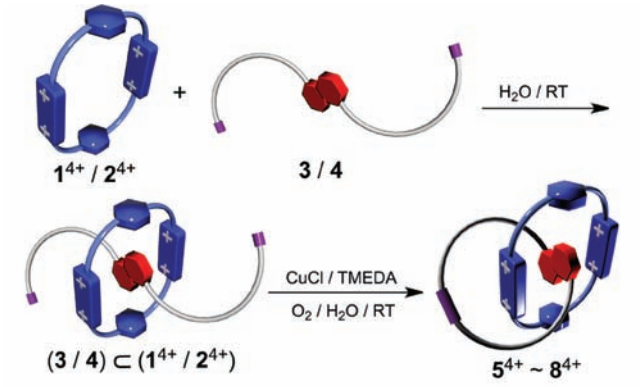

Compound Number	Acceptor	Donor	Isolated Yield (%)
$\mathbf{5}^{4+}$			63
$\mathbf{6}^{4+}$			51
$\mathbf{7}^{4+}$			34
$\mathbf{8}^{4+}$			40

cyclization in aqueous media was the choice of the Glaser−Hay oxidative coupling reaction[25,26] which can be performed efficiently in water. Under these conditions, the triple bonds undergo intramolecular homocoupling while threaded through the cavities of the tetracationic cyclophanes, thus affording the [2]catenanes $\mathbf{5}^{4+}$−$\mathbf{8}^{4+}$. In **3** and **4**, triethylene glycol spacers were employed between the naphthalene units and the propargyl functions, since they provide[24] the optimum length for the formation of macrocycles, templated by the tetracationic cyclophanes.

In aprotic organic solvents, the binding affinities of $\mathbf{1}^{4+}$ and $\mathbf{2}^{4+}$ with **3** and **4** rely on a combination of [$\pi\cdots\pi$] and [C−H$\cdots$O] interactions. Although the H-bonding is suppressed in water, the inner cavities of the cyclophanes serve as hydrophobic pockets for the nonpolar naphthalene ring systems. In fact, such strong hydrophobic interactions not only compensate for the loss of the binding affinity contributed from H-bonds but also actually elevate the corresponding binding constants by orders of magnitude compared to those observed in organic solvents. For example, the binding affinities of $\mathbf{2}^{4+}$ toward dioxynaphthalene derivatives in water[21] are around 10^6 M^{-1}, compared with 10^3−10^4 M^{-1} in MeCN.[27] The binding constant[28] of $\mathbf{3}\subset\mathbf{1}^{4+}$ in aqueous solution is even higher (6×10^7 M^{-1}), probably because of the more extensive π-faces provided by the DAP^{2+} units in compound $\mathbf{1}^{4+}$. Such a high binding constant ensures an efficient template effect for the all-important next step of the synthesis in water, leading to the production of the [2]catenanes. Although **3** and **4** are sparingly soluble in water, we found that mixing a large excess of **3/4** with $\mathbf{1}^{4+}$ in D_2O affords a deep red/green colored[29] solution after sonication. The ^1H NMR spectra of these mixtures reveal[30] the quantitative formation of the 1:1 host−guest inclusion complexes $\mathbf{3}\subset\mathbf{1}^{4+}$ or $\mathbf{4}\subset\mathbf{1}^{4+}$ [see Supporting Information (SI), Figure S5]. As a result, in order to carry out a homogeneous reaction in water, it is not necessary to add organic solvent or to attach additional solubilizing groups onto **3** or **4**. It should be noted that the proton resonances for $\mathbf{1}^{4+}$ in its complexed form were separated into two distinct sets of signals compared to those in the free $\mathbf{1}^{4+}$. The peak separations ($H_\alpha/H_{\alpha'}$, $H_\gamma/H_{\gamma'}$, $H_a/H_{a'}$, and $H_b/H_{b'}$ in Figure 2) which occur during the complexation are[31] a result of the 1,5-disubstituted naphthalene units imposing their local C_2-axis of symmetry on the tetracationic cyclophanes.[32]

With the well-characterized supramolecular complexes in hand, we continued to pursue the syntheses of the corresponding [2]catenanes. For example, the self-assembly of the [2]pseudorotaxane $\mathbf{3}\subset\mathbf{1}^{4+}$ preorganized the components to undergo an intramolecular oxidative coupling, affording the target [2]catenane $\mathbf{5}^{4+}$. This reaction proceeds under Glaser−Hay conditions[26] in water, involving oxygen, CuCl, and tetramethylethylenediamine (TMEDA). At room temperature, bubbling air into the reaction mixture facilitated the completion of the catenation within 2 h. Analytical high performance liquid chromatography (HPLC) on the reaction mixture revealed (see SI, Figure S1) an almost quantitative conversion of the pseudorotaxane to the corresponding [2]catenane. The product $\mathbf{5}^{4+}$ was purified by preparative HPLC to afford the trifluoroacetate salt $\mathbf{5}\cdot 4CF_3CO_2$ in 63% isolated yield. Using the same protocol, we were able to obtain[33] (Scheme 1) catenanes $\mathbf{6}\cdot 4CF_3CO_2$ (51%), $\mathbf{7}\cdot 4CF_3CO_2$ (34%), and $\mathbf{8}\cdot 4CF_3CO_2$ (40%). All these products were fully characterized (see SI, Section 2) by ^1H and ^{13}C NMR spectroscopies and by mass spectrometries.

Single crystals of $\mathbf{5}^{4+}$ and $\mathbf{8}^{4+}$ suitable for X-ray diffraction were grown by slow vapor diffusion of *i*-Pr_2O into a solution of $\mathbf{5}\cdot 4PF_6$ or $\mathbf{8}\cdot 4CF_3CO_2$ in MeCN, respectively. Their crystal structures are shown[34] in Figure 2. According to the crystal structure of $\mathbf{5}^{4+}$, the butadiyne-triethylene glycol loop encircles one of the DAP^{2+} units assisted by the weak [$\pi\cdots\pi$] interaction between the butadiyne unit and the DAP^{2+} unit (distance ~3.37 Å). This fact illustrates the reality that the two DAP^{2+} units in $\mathbf{5}^{4+}$ experience distinctively different chemical environments. Moreover, H-bond formation between the oxygen atoms of the glycol chain and H_a, H_α, and H_γ was also observed in the solid state, e.g., a short distance (2.16 Å) between H_α and the third oxygen in the glycol chain (red dotted line in Figure 2).

In the solution phase the molecular motion becomes apparent. We propose a "pirouetting" motion (Figure 3) brought about by the ability of butadiyne unit to interact with both DAP^{2+} units. Presumably, pirouetting of the butadiyne-triethylene glycol loop should be fast enough at high temperatures to bring about the coalescence of the ^1H NMR signals arising from these two different types of DAP^{2+} units. Upon lowering the temperature, however, this movement can be slowed down on the ^1H NMR time scale and the resonances of the two DAP^{2+} units can therefore be distinguished. Indeed, variable temperature ^1H NMR spectra of $\mathbf{5}\cdot 4CF_3CO_2$ recorded within the range 274−333 K showed (Figure 3a) temperature dependences for the resonances associated with both H_α and $H_{\alpha'}$, as well as for one of the H_γ and H_b protons. These

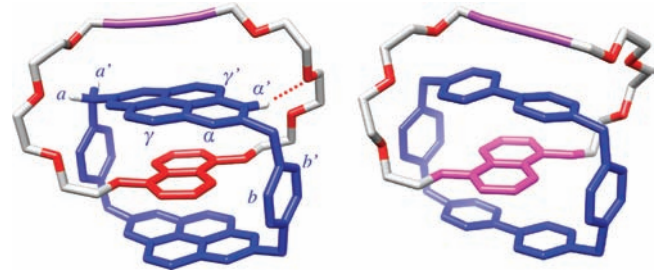

Figure 2. Solid-state structure of $\mathbf{5}^{4+}$ (left) and $\mathbf{8}^{4+}$ (right). In addition to the disordered PF_6^- or $CF_3CO_2^-$ counterions, hydrogen atoms and solvent molecules are omitted for the sake of clarity.

protons undergo coalescences at temperatures (T_c) in the range 295−308 K. Rotating frame Overhauser Spectroscopy (ROESY) showed (see SI, Figure S11) positive-phased correlations between the separated peaks at low temperature, corroborating the fact that these separated signals belong to the same protons but are slowly exchanging with each other. Such signal coalescence confirmed our hypothesis[31,35] on the pirouetting movement (Figure 3b, see SI, Figure S7 and Table S2) of the butadiyne-triethylene glycol loop.

According to the T_c values for the different proton probes, the energy barriers ($\Delta G^{\ddagger}$) for such pirouetting movement in water at the corresponding coalescent temperatures were calculated (see SI, Table S1). The activation enthalpy ($\Delta H^{\ddagger}$) and entropy ($\Delta S^{\ddagger}$) in water were determined to be (Table 1) 7.4 kcal·mol^{-1} and −23.6 cal·mol^{-1}·K^{-1}, respectively. In order to compare the molecular motion in water to that in organic solvents, we performed similar VT NMR measurements (see SI, Figure S7 and Table S2) on $\mathbf{5}^{4+}$ in aprotic organic solvents such as CD_3CN. Other coalescence phenomena were observed in keeping with this pirouetting motion. We believe that the higher $\Delta H^{\ddagger}$ (11.2 kcal·mol^{-1}) in CD_3CN represents the increased enthalpy cost in breaking the H-bonds in order to render the transition state of the pirouetting movement,

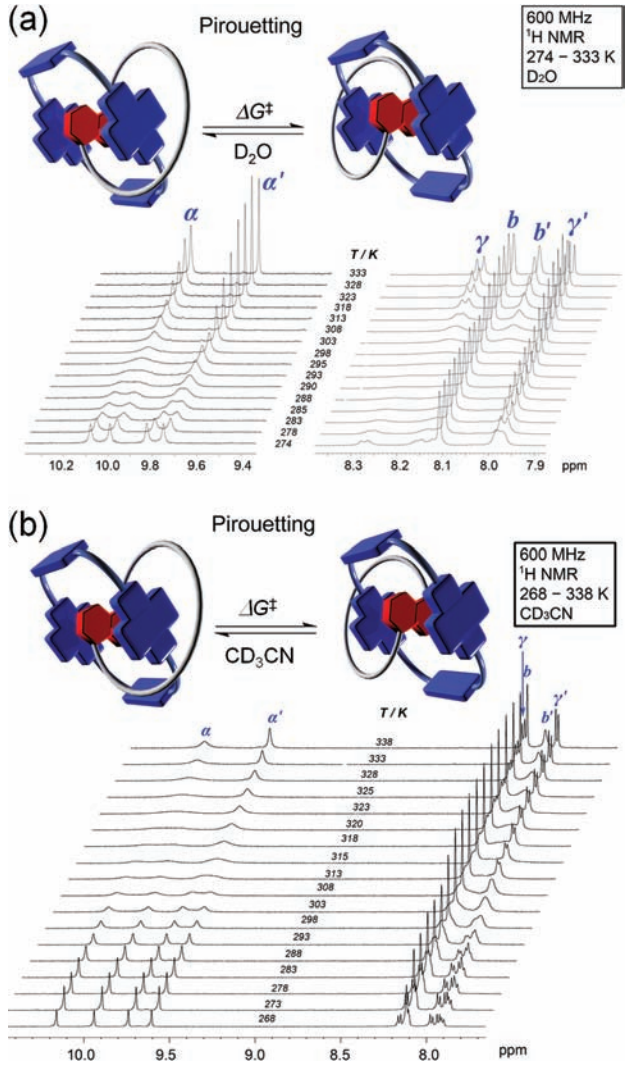

Figure 3. (a) Partial 600 MHz ^{1}H NMR spectra recorded in D_2O at different temperatures displaying the coalescence of the signals for four sets of probe protons identified in $\mathbf{5}^{4+}$ in Figure 2. (b) Partial 600 MHz ^{1}H NMR spectra recorded in CD_3CN at different temperatures displaying the coalescence of the signals for three sets of probe protons identified in $\mathbf{5}^{4+}$.

Table 1. Kinetic Parameters[a] of the Pirouetting Motion Obtained from Temperature-Dependent ^{1}H NMR Spectra Recorded on the [2]Catenane $\mathbf{5}^{4+}$ in D_2O and in CD_3CN

Solvent	$\Delta H^{\ddagger}$ (kcal·mol^{-1})[b]	$\Delta S^{\ddagger}$ (cal·mol^{-1}·K^{-1})[b]	$\Delta G^{\ddagger}$ at 298 K (kcal·mol^{-1})[b]
D_2O	7.4	−23.6	14.4
CD_3CN	11.2	−12.7	15.0

[a] Derived from the data shown in Tables S1 and S2 in the SI. [b] Value ± 0.1.

while the less negative $\Delta S^{\ddagger}$ (−12.7 cal·mol^{-1}·K^{-1}) in CD_3CN can be attributed to the weaker solvation effect of the butadiyne-triethylene glycol loop with CD_3CN solvent molecules compared to that of D_2O. Moreover, VT NMR spectra of $\mathbf{6}^{4+}$ and $\mathbf{7}^{4+}$ in water showed no peak separation at low temperature (see SI, Figures S8−S9), indicating that the butadiyne-triethylene glycol loops in $\mathbf{6}^{4+}$ and in $\mathbf{7}^{4+}$ were pirouetting at a rate too fast to be measured even at a temperature close to the freezing point of D_2O. The difference between the rates of pirouetting of $\mathbf{5}^{4+}$ and $\mathbf{6}^{4+}$ is probably a consequence of the larger steric bulk of the DAP^{2+} units in $\mathbf{5}^{4+}$ compared to the less bulky $BIPY^{2+}$ units in $\mathbf{6}^{4+}$.

In summary, the syntheses of charged donor−acceptor [2]catenanes in water have been achieved under kinetic control in high conversions. The template-directed approach involves a Cu(I)-catalyzed oxidative coupling of dialkynyl threads under the templation of tetracationic cyclophanes. Dynamic ^{1}H NMR spectroscopy demonstrates the pirouetting motion of the butadiyne-triethylene glycol loop around the cyclophane for $\mathbf{5}^{4+}$ in both aqueous and organic solvents. These results open up the way to the "in-water" synthesis and investigation of more complex functional molecular switches and machines in the future. Such artificial actuators could be used as molecular prosthetics[36] and so hold promise for controlling biological processes using correlated molecular motions at the nanoscale level.

Acknowledgment. The authors acknowledge support from the Air Force Office of Scientific Research (AFOSR) under the Multidisciplinary Research Program of the University Research Initiative (MURI), Award FA9550-07-1-0534 entitled "Bioinspired Supramolecular Enzymatic Systems". L.F. acknowledges the support of a Ryan Fellowship and a Non-Equilibrium Research Center Fellowship from Northwestern University (NU). A.C.F. acknowledges support from an NSF Graduate Research Fellowship. We thank Ms. Charlotte L. Stern and Dr. Amy A. Sarjeant at NU for collecting and solving X-ray crystallographic data.

Supporting Information Available: Experimental details and spectral characterization data. This material is available free of charge via the Internet at http://pubs.acs.org.

References

(1) Aristotle *Metaphysics*.
(2) Chaplin, M. *Nat. Rev. Mol. Cell Biol.* **2006**, *7*, 861–866.
(3) (a) Gresser, M. J.; Myers, J. A.; Boyer, P. D. *J. Biol. Chem.* **1982**, *257*, 12030–12038. (b) Noji, H.; Yasuda, R.; Yoshida, M.; Kinosita, K., Jr. *Nature* **1997**, *386*, 299–302. (c) Yasuda, R.; Noji, H.; Yoshida, M.; Kinosita, K., Jr.; Itoh, H. *Nature* **2001**, *410*, 898–904. (d) Itoh, H.; Takahashi, A.; Adachi, K.; Noji, H.; Yasuda, R.; Yoshida, M.; Kinosita, K., Jr. *Nature* **2004**, *427*, 465–468. (e) Watanabe, R.; Iino, R.; Noji, H. *Nature Chem. Biol.* **2010**, *6*, 814–820.
(4) (a) Kull, F. J.; Sablin, E. P.; Lau, R.; Fletterick, R. J.; Vale, R. D. *Nature* **1996**, *380*, 550–555. (b) Hirokawa, N.; Noda, Y.; Tanaka, Y.; Niwa, S. *Nature Rev. Mol. Cell. Biol.* **2010**, *10*, 682–696. (c) Sindelar, C. V.; Downing, K. H. *Proc. Natl. Acad. Sci. U.S.A* **2010**, *107*, 4111–4116.
(5) (a) Pollard, T. D.; Shelton, E.; Weihing, R. R.; Korn, E. D. *J. Mol. Biol.* **1970**, *50*, 91–97. (b) Finer, J. T.; Simmons, R. M.; Spudich, J. A. *Nature* **1994**, *368*, 113–119. (c) Sweeney, H. L.; Houdusse, A. *Annu. Rev. Biophys.* **2010**, *39*, 539–557.
(6) Astumian, R. D.; Derényi, I. *Biophys. J.* **1999**, *77*, 993–1002.
(7) (a) Balzani, V.; Credi, A.; Raymo, F. M.; Stoddart, J. F. *Angew. Chem.*,

Int. Ed. **2000**, *39*, 3348–3391. (b) Horinek, D.; Michl, J. *Proc. Natl. Acad. Sci. U.S.A.* **2005**, *102*, 14175–14180. (c) Kay, E. R.; Leigh, D. A.; Zerbetto, F. *Angew. Chem., Int. Ed.* **2007**, *46*, 72–191. (d) Feringa, B. L. *J. Org. Chem.* **2007**, *72*, 6635–6652.
(8) Oshovsky, G. V.; Reinhoudt, D. N.; Verboom, W. *Angew. Chem., Int. Ed.* **2007**, *46*, 2366–2393.
(9) (a) Dietrich-Buchecker, C. O.; Sauvage, J.-P. *Angew. Chem., Int. Ed.* **1989**, *28*, 189–192. (b) Vickers, M. S.; Beer, P. D. *Chem. Soc. Rev.* **2007**, *36*, 211–225. (c) Stoddart, J. F.; Colquhoun, H. M. *Tetrahedron* **2008**, *64*, 8231–8263. (d) Fang, L.; Olson, M. A.; Benítez, D.; Tkatchouk, E.; Goddard, W. A., III; Stoddart, J. F. *Chem. Soc. Rev.* **2010**, *39*, 17–29.
(10) (a) Asakawa, M.; Ashton, P. R.; Balzani, V.; Credi, A.; Hamers, C.; Mattersteig, G.; Montalti, M.; Shipway, A. N.; Spencer, N.; Stoddart, J. F.; Tolley, M. S.; Venturi, M.; White, A. J. P.; Williams, D. J. *Angew. Chem., Int. Ed.* **1998**, *37*, 333–337. (b) Fang, L.; Hmadeh, M.; Wu, J.; Olson, M. A.; Spruell, J. M.; Trabolsi, A.; Yang, Y.-W.; Elhabiri, M.; Albrecht-Gary, A.-M.; Stoddart, J. F. *J. Am. Chem. Soc.* **2009**, *131*, 7126–7134. (c) Coskun, A.; Wesson, P. J.; Klajn, R.; Trabolsi, A.; Fang, L.; Olson, M. A.; Dey, S. K.; Grzybowski, B. A.; Stoddart, J. F. *J. Am. Chem. Soc.* **2010**, *132*, 4310–4320.
(11) (a) Anderson, S.; Anderson, H. L.; Sanders, J. K. M. *Acc. Chem. Res.* **1993**, *26*, 469–475. (b) Hubin, T. J.; Busch, D. H. *Coord. Chem. Rev.* **2000**, *200*, 5–52. (c) Diederich, F.; Stang, P. J. *Template-Directed Synthesis*; Wiley-VCH: Weinheim, 2006. (d) Meyer, C. D.; Joiner, C. S.; Stoddart, J. F. *Chem. Soc. Rev.* **2007**, *36*, 1705–1723. (e) Griffiths, K. E.; Stoddart, J. F. *Pure Appl. Chem.* **2008**, *80*, 485–506.
(12) Armspach, D.; Ashton, P. R.; Moore, C. P.; Spencer, N.; Stoddart, J. F.; Wear, T. J.; Williams, D. J. *Angew. Chem., Int. Ed.* **1993**, *32*, 854–858.
(13) Ashton, P. R.; Goodnow, T. T.; Kaifer, A. E.; Reddington, M. V.; Slawin, A. M. Z.; Spencer, N.; Stoddart, J. F.; Vicent, C.; Williams, D. J. *Angew. Chem., Int. Ed.* **1989**, *28*, 1396–1399.
(14) (a) Vögtle, F.; Meier, S.; Hoss, R. *Angew. Chem., Int. Ed.* **1992**, *31*, 1619–1622. (b) Johnston, A. G.; Leigh, D. A.; Pritchard, R. J.; Deegan, M. D. *Angew. Chem., Int. Ed.* **1995**, *34*, 1209–1212. (c) Ashton, P. R.; Campbell, P. J.; Chrystal, E. J. T.; Glink, P. T.; Menzer, S.; Philp, D.; Spencer, N.; Stoddart, J. F.; Tasker, P. A.; Williams, D. J. *Angew. Chem., Int. Ed.* **1995**, *34*, 1865–1869.
(15) (a) Dietrich-Buchecker, C. O.; Sauvage, J.-P. *Tetrahedron Lett.* **1983**, *24*, 5095–5098. (b) Dietrich-Buchecker, C. O.; Sauvage, J.-P. *J. Am. Chem. Soc.* **1984**, *106*, 3043–3045. (c) Sauvage, J.-P. *Acc. Chem. Res.* **1990**, *23*, 319–327. (d) Piguet, C.; Bernardinelli, G.; Williams, A. F.; Bocquet, B. *Angew. Chem., Int. Ed.* **1995**, *34*, 582–584. (e) Leigh, D. A.; Lusby, P. J.; Teat, S. J.; Wilson, A. F.; Wong, J. K. Y. *Angew. Chem., Int. Ed.* **2001**, *40*, 1538–1543.
(16) (a) Harada, A.; Li, J.; Kamachi, M. *Nature* **1992**, *356*, 325–327. (b) Craig, M. R.; Hutchings, M. G.; Claridge, T. D. W.; Anderson, H. L. *Angew. Chem., Int. Ed.* **2001**, *40*, 1071–1074. (c) Zhao, Y.-L.; Dichtel, W. R.; Trabolsi, A.; Saha, S.; Aprahamian, I.; Stoddart, J. F. *J. Am. Chem. Soc.* **2008**, *130*, 11294–11296.
(17) Fujita, M.; Ibukuro, F.; Hagihara, H.; Ogura, K. *Nature* **1994**, *367*, 720–723.
(18) (a) Au-Yeung, H. Y.; Pantoş, G. D.; Sanders, J. K. M. *Proc. Natl. Acad. Sci. U.S.A.* **2009**, *106*, 10466–10470. (b) Au-Yeung, H. Y.; Pantoş, G. D.; Sanders, J. K. M. *Angew. Chem., Int. Ed.* **2010**, *49*, 5331–5334.
(19) (a) Odell, B.; Reddington, M. V.; Slawin, A. M. Z.; Spencer, N.; Stoddart, J. F.; Williams, D. J. *Angew. Chem., Int. Ed.* **1988**, *27*, 1547–1550. (b) Ashton, P. R.; Boyd, S. E.; Brindle, A.; Langford, S. J.; Menzer, S.; Pérez-García, L.; Preece, J. A.; Raymo, F. M.; Spencer, N.; Stoddart, J. F.; White, A. J. P.; Williams, D. J. *New J. Chem.* **1999**, *23*, 587–602. (c) Sue, C.-H.; Basu, S.; Fahrenbach, A. C.; Shveyd, A. K.; Dey, S. K.; Botros, Y. Y.; Stoddart, J. F. *Chem. Sci.* **2010**, *1*, 119–125.
(20) Bernardo, A. R.; Stoddart, J. F.; Kaifer, A. E. *J. Am. Chem. Soc.* **1992**, *114*, 10624–10631.
(21) (a) Venturi, M.; Dumas, S.; Balzani, V.; Cao, J.; Stoddart, J. F. *New J. Chem.* **2004**, *28*, 1032–1037. (b) Bria, M.; Cooke, G.; Cooper, A.; Garety, J. F.; Hewage, S. G.; Nutley, M.; Rabani, G.; Woisel, P. *Tetrahedron Lett.* **2007**, *48*, 301–304.
(22) Miljanić, O. Š.; Dichtel, W. R.; Mortezaei, S.; Stoddart, J. F. *Org. Lett.* **2006**, *8*, 4835–4838.
(23) (a) Hamilton, D. G.; Prodi, L.; Feeder, N.; Sanders, J. K. M. *J. Chem. Soc., Perkin Trans. 1* **1999**, 1057–1065. (b) Crowley, J. D.; Goldup, S. M.; Gowans, N. D.; Leigh, D. A.; Ronaldson, V. E.; Slawin, A. M. Z. *J. Am. Chem. Soc.* **2010**, *132*, 6243–6248.
(24) Miljanić, O. Š.; Dichtel, W. R.; Khan, S. I.; Mortezaei, S.; Heath, J. R.; Stoddart, J. F. *J. Am. Chem. Soc.* **2007**, *129*, 8236–8246.
(25) Eglinton, G.; Galbraith, A. R. *J. Chem. Soc.* **1959**, 889–896.
(26) (a) Hay, A. S. *J. Org. Chem.* **1962**, *27*, 3320–3321. (b) Fomina, L.; Vazquez, B.; Tkatchouk, E.; Fomine, S. *Tetrahedron* **2002**, *58*, 6741–6747.
(27) Choi, J. W.; Flood, A. H.; Steuerman, D. W.; Nygaard, S.; Braunschweig, A. B.; Moonen, N. N. P.; Laursen, B. W.; Luo, Y.; DeIonno, E.; Peters, A. J.; Jeppesen, J. O.; Xu, K.; Stoddart, J. F.; Heath, J. R. *Chem.—Eur. J.* **2006**, *12*, 261–279.
(28) The binding constant was determined by fluorescence titration between **1**·4CF_3CO_2 and **3**. For details, see SI.
(29) The complex **3**⊂$\mathbf{1}^{4+}$ reveals a deep red color (λ_{max} = 520 nm), while **4**⊂$\mathbf{1}^{4+}$ is deep green (λ_{max} = 685 nm). These colors originate from the charge transfer band between the cylcophane $\mathbf{1}^{4+}$ and dioxynaphthalene or diaminonaphthalene, respectively. For the spectra, see SI, Figure S12.
(30) Although an excess of **3** or **4** was added into the solution, uncomplexed **3**/**4** cannot be observed in the ^{1}H NMR spectra because of the poor solubility of **3** and **4** in D_2O.
(31) Vignon, S. A.; Stoddart, J. F. *Collect. Czech. Chem. Commun.* **2005**, *70*, 1493–1576.
(32) Since the 180° rotation around its O···O axis of the naphthalene unit is slow on the ^{1}H NMR timescale, the differences between H_a and $H_{a'}$ et al. can be distinguished by ^{1}H NMR spectroscopy. In fact, the rate of this "out-in, turn it around" movement is persistently slow on the ^{1}H NMR timescale, even at the elevated temperature of 313 K (see SI).
(33) An excess of **3** or **4** was added to a solution of **1**·4CF_3CO_2 or **2**·4CF_3CO_2 (20.6 μmol) in D_2O (1 mL). The reaction mixture was sonicated for 5 min, before being stirred for 1 h, at which point the ^{1}H NMR spectrum indicated 100% complexation. The solution was then added into an aqueous solution of CuCl (0.6 mmol) and tetramethylethylenediamine (TMEDA) (0.5 mL). Air was bubbled into the reaction mixture in order to introduce oxygen. Analytical HPLC indicated >90% conversion after 1 h. The solution was filtered before saturated aqueous NH_4PF_6 solution was added to the filtrate. The resulting precipitate was collected and washed with H_2O (3 × 5 mL). Preparative reversed-phase HPLC (C_{18}; MeCN−H_2O/0−35% in 40 min then 35−100% in 10 min, with 0.1% CF_3CO_2H) was performed, and the pure fractions were collected. The pure product was obtained as a crystalline solid after removing the solvent. We hypothesize that the lower isolated yields of $\mathbf{7}^{4+}$ and $\mathbf{8}^{4+}$ arise from nucleophilic attack of the amino groups upon the strained methylenes of the cyclophanes. See ref 19c. **5**·4CF_3CO_2: Deep red solid (63%). ^{1}H NMR (600 MHz, D_2O, 323 K) δ = 1.42 (d, J = 7.8 Hz, 2H), 3.41 (t, J = 4.2 Hz, 4H), 3.48 (br, 4H), 3.58−3.59 (m, 4H), 3.67−3.68 (m, 4H), 3.78 (br, 4H), 3.95 (br, 4H), 4.06 (t, J = 4.2 Hz, 4H), 5.45 (t, J = 7.8 Hz, 2H), 5.64 (d, J = 8.4 Hz, 2H), 6.19 (s, 8H), 7.98 (d, J = 9.0 Hz, 4 H), 8.05 (s, 4H), 8.11 (s, 4H), 8.18 (d, J = 9.0 Hz, 4H), 9.68 (s, 4H), 9.98 (s, 4H). ^{13}C NMR (125 MHz, D_2O, 298 K) δ = 21.8, 58.1, 61.1, 67.5, 67.6, 68.7, 70.0, 70.5, 70.6, 71.2, 71.5, 72.2, 74.0, 105.6, 116.9 (q, J = 290 Hz), 121.4, 124.8, 126.1, 129.4, 132.1, 136.9, 149.9, 163.6 (q, J = 36 Hz). ESI-MS: calcd for $[M-2HPF_6-PF_6]^+$ m/z = 1257.4501, found m/z = 1257.4548; calcd for $[M-2PF_6]^{2+}$ m/z = 702.2071, found m/z = 702.2094; calcd for $[M-HPF_6-2PF_6]^{2+}$ m/z = 629.2250, found m/z = 629.2222. **6**·4CF_3CO_2: Purple solid (51%); for characterization data, see ref 24. **7**·4CF_3CO_2: Dark green solid (34%). ^{1}H NMR (600 MHz, D_2O, 313 K) δ = 0.42 (d, J = 7.8 Hz, 2H), 3.16−3.17 (m, 4H), 3.42−3.43 (m, 4H), 3.50 (s, 4H), 3.79−3.80 (m, 4H), 4.06−4.08 (m, 4H), 4.15 (br, 4H), 4.20 (br, 4H) 5.31 (d, J = 7.8 Hz, 2H), 5.44 (t, J = 7.8 Hz, 2H), 6.13−6.20 (m, 8H), 7.91 (d, J = 9.0 Hz, 4H), 8.05 (s, 4H), 8.08 (d, J = 9.0 Hz, 4H), 9.66 (s, 4H), 9.99 (s, 4H). ^{13}C NMR (125 MHz, D_2O, 298 K) δ = 48.7, 66.5, 69.3, 69.5, 69.9, 70.5, 70.8, 73.3, 99.2, 104.1, 116.9 (q, J = 290 Hz), 123.0, 123.9, 127.2, 127.5, 128.9, 130.4, 132.4, 134.3, 136.5, 138.0, 138.8, 141.1, 163.6 (q, J = 36 Hz). ESI-MS: calcd for $[M-2CF_3CO_2]^{2+}$ m/z = 669.2245, found m/z = 669.2456; calcd for $[M-CF_3CO_2H-2CF_3CO_2]^{2+}$ m/z = 612.2517, found 612.2491. **8**·4CF_3CO_2: Emerald green solid (40%). ^{1}H NMR (500 MHz, D_2O, 298 K) δ = 1.47 (d, J = 8.5 Hz, 2H), 3.42 (br, 4H), 3.54 (br, 4H), 3.69 (br, 4H), 3.76 (s, 4H), 3.93 (br, 4H), 4.04 (br, 8H), 5.81−5.85 (m, 8H), 6.06 (d, J = 8.5 Hz, 2H), 6.13 (t, J = 8.5 Hz, 2H), 7.38 (d, J = 4.5 Hz, 4H), 7.50 (d, J = 4.5 Hz, 4H), 8.04 (s, 4H), 8.07 (s, 4H), 8.92 (d, J = 6.0 Hz, 4H), 9.16 (d, J = 6.0 Hz, 4H). ^{13}C NMR (150 MHz, D_2O, 298 K) δ = 43.4, 58.0, 65.0, 68.9, 69.5, 69.9, 70.4, 70.8, 74.9, 102.7, 102.8, 115.4, 117.2 (q, J = 290 Hz), 121.5, 124.7, 125.9, 128.2, 130.2, 131.9, 137.2, 140.6, 143.3, 144.5, 145.0, 163.0 (q, J = 36 Hz). ESI-MS: calcd for $[M-CF_3CO_2]^+$ m/z = 1355.4730, found m/z = 1355.4743; calcd for $[M-2CF_3CO_2]^{2+}$ m/z = 621.2445, found m/z = 621.2465.
(34) Crystal parameters for **5**·4PF_6: $C_{158}H_{153}F_{48}N_{15}O_{16}P_8$, M = 3677.71, Triclinic, a = 13.7023(2) Å, b = 14.0842(3) Å, c = 23.0481(4) Å, α = 84.632(1)°, β = 76.883(1)°, γ = 68.292(1)°, U = 4024.47(13) Å^3, T = 113(2) K, space group $P\bar{1}$, Z = 1, ρ = 1.517 g·cm^{-3}. Crystal parameters for **8**·4CF_3CO_2: $C_{80}H_{78}F_{12}N_{10}O_{14}$, M = 3263.04, Triclinic, a = 13.7694(6) Å, b = 14.0822(8) Å, c = 21.3390(12) Å, α = 82.096(5)°, β = 88.638(4)°, γ = 69.667(4)°, V = 3841.7(3) Å^3, T = 100(2) K, space group $P\bar{1}$, Z = 1, ρ = 1.410 g·cm^{-3}. CCDC 794118 and 794119 contains the supplementary crystallographic data for this paper. These data can be obtained free of charge from the Cambridge Cyrstallographic Data Centre (CCDC) via www.ccdc.cam.ac.uk/ data_request/cif.
(35) Coskun, A.; Friedman, D. C.; Li, H.; Patel, K.; Khatib, H. A.; Stoddart, J. F. *J. Am. Chem. Soc.* **2009**, *131*, 2493–2495.
(36) (a) Chilkoti, A.; Chen, G.; Stayton, P. S.; Hoffman, A. S. *Bioconjugate Chem.* **1994**, *5*, 504–507. (b) Shimoboji, T.; Larenas, E.; Fowler, T.; Kulkarni, S.; Hoffman, A. S.; Stayton, P. S. *Proc. Natl. Acad. Sci. U.S.A.* **2002**, *99*, 16592–16596.

JA1087562